Available online at www.sciencedirect.com
ScienceDirect
Ultrasonics Sonochemistry 15 (2008) 55–64
Ultrasonics SONOCHEMISTRY
www.elsevier.com/locate/ultsonch

Experimental investigations on ultrasound mediated particle breakage

Vinay Raman [b], Ali Abbas [a,*]

[a] School of Chemical and Biomedical Engineering, Nanyang Technological University, Singapore
[b] Department of Chemical Engineering, Indian Institute of Technology Madras, India

Received 6 July 2006; received in revised form 11 October 2006; accepted 6 November 2006
Available online 3 February 2007

Abstract

This paper investigates the effect of high-intensity ultrasound on the breakage characteristics of particles suspended in water. A continuous sonicated flow experimental apparatus is used involving a 24 kHz horn type transducer and continuous in-line particle chord length measurement. The effects of sonication power (150–350 W) and temperature (10–50 °C) on the breakage characteristics are investigated. Higher breakage is favored at higher sonication power. An optimum temperature in the range tested is observed to exist between 25 °C and 37 °C. The acoustic cavitation field is influenced by temperature through a complex interplay of vapor pressure, surface tension and viscosity leading to the optimum observed in particle breakage. The efficiency of ultrasound energy conversion to particle breakage is calculated using calorimetry and found along with the net breakage efficiency to initially increase with temperature followed by a decrease after the optimum. It is found to be independent of input ultrasonic power. The effects of contact time is also investigated.

Keywords: Ultrasound; Particle breakage; Breakage kinetics; Chord length distributions; Focused beam reflectance measurement

1. Introduction

Ultrasonic cavitation is the phenomenon by which a time-varying acoustic wave when induced into a liquid medium ruptures the liquid apart during the rarefaction cycle, creating transient or stable acoustic cavities (bubbles). The transient cavitations end up in collapse, within a short span of time, resulting in shock waves, while stable cavitations resonate in the applied sound field, surviving the local pressure variations for a number of acoustic cycles. The cavitation forces induced during transient collapse of cavitating bubbles are of great importance and are known to cause many chemical and physical effects, e.g., lysis of solvent molecules resulting in formation of free radicals, augmentation of chemical reaction rates [1], mechanical effects like erosion of solid surfaces or pitting [1–4], dispersion of agglomerated powders in solution [5] and particle breakage [6] which is the focus of the present study.

The beneficial effects of high-intensity ultrasound (HIU) on particle breakage have been exploited in the field of catalysis where the ultrasonic collision test has evolved as a standard test to characterize the breakage resistance of catalyst particles [7,8]. The effect of HIU on inorganic solids was previously studied, where a dramatic rise in reactivity was attributed to particle breakage [6]. It has been generally recognized that HIU is effective for comminution (i.e., size reduction) of particles. It is further reported that, unlike grinding comminution operations that yield new particle properties such as those related to surface charge modifications, sonication does not alter the crystalline structure [9]. The production of sub-micron talc particles by HIU was previously reported and resulted in the attainment of a narrow size distribution [10]. It is of significance to elucidate the effect of operational conditions if one is to arrive at optimal HIU particle breakage. Towards this goal, a recent study examining the energy requirements for particle size reduction by HIU was performed [11],

* Corresponding author. Current address: Division of Engineering Science and Technology, University of New South Wales Asia, Singapore. Tel.: +65 6304 1426; fax: +65 6472 2849.
E-mail address: aabbas@unswasia.edu.sg (A. Abbas).

1350-4177/$ - see front matter © 2007 Elsevier B.V. All rights reserved.
doi:10.1016/j.ultsonch.2006.11.009

while in [12], the effects of sonication power, sonication time and loading on particle breakage were discussed.

It is expected that operational conditions namely, sonication power, contact time and temperature play important roles in the particle breakage. The sonication power influences the level of cavitation in the fluid. At higher power levels, the number of cavitation events increases because larger numbers of transient cavitation bubbles are formed, hence influencing the magnitude of breakage. Contact time is the duration of exposure of the particles to the ultrasound. Particles exposed to longer durations of sonication are expected to observe increased levels of breakage. Temperature has a significant effect on the ultrasonic field; it alters the viscosity, density and vapor pressure of the medium, thereby affecting a change in the cavitation threshold [1,4]. If transient cavitation collapse is sought as one of the main affectors of particle breakage, then temperature would be expected to have a strong impact. There have been contradictory reports on the effect of temperature on power transfer capability of the ultrasonic system. Some claim, constancy of specific input power with temperature of operation [13,14] while others, claim a decrease in specific input power with increase in temperature [15]. An independent study is made in this paper to verify the effect of temperature on ultrasonic power transfer.

Ultrasound energy conversion into specific desirable effects is very important from the industrial viewpoint [16,17]. There are very few reports in the literature which discuss this issue. Kuijpers et al. have studied the effect of characteristic parameters of ultrasonic system viz., amplitude ratio (input power) and temperature on the efficiency of ultrasound energy conversion to radical formation [14].

Studies that discuss either the effect of temperature on particle breakage kinetics or the efficiency of ultrasound energy conversion to ultrasonic mediated particle breakage, seem to be absent from the literature. We thus take up these issues for discussion in this paper via rigorous experimental parametric investigations using aluminium oxide (Al_2O_3) particles as the primary model particle system. Such a study would be very relevant to industrial scale-up strategies as well as being useful in elucidating particle breakage at the phenomenological level.

2. Experimental

2.1. Materials

Aluminium oxide particles were used for this study, consisting of finely hand ground and sieved particles with mean nominal size of 150 μm. Samples were prepared by firstly grinding in a mortar standard grade Al_2O_3 pellets before sieving using standard sieves (Advantec, Sonic Sifter). The roundness index of the particles was determined by image analysis and was found to be 0.72.

2.2. Ultrasonic equipment

Sonication was performed using a 24 kHz horn type transducer (Sartorius, Labsonic, Germany) capable of delivering a maximum of 450 W of power. A continuous flow apparatus was setup as shown in Fig. 1 consisting of a variable speed peristaltic pump (Watson Marlow, USA), ultrasonic transducer fitted inside a jacketed glass reactor, focused beam reflectance measurement (FBRM)

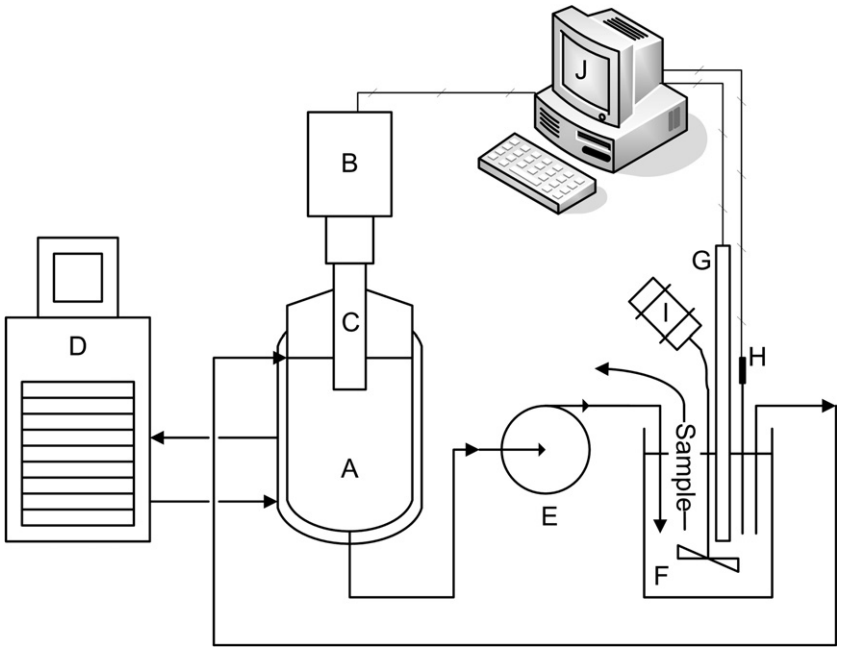

Fig. 1. Experimental Setup: (A) sonication vessel, (B) ultrasonic transducer, (C) ultrasonic probe, (D) temperature control system, (E) peristaltic pump, (F) FBRM beaker, (G) FBRM probe, (H) Pt100, (I) agitator, and (J) computer (data acquisition).

probe (Mettler–Toledo Lasentec Products, USA), temperature control system (Lauda, Germany), and a computer for data acquisition. The peristaltic pump, capable of creating pressure head to maintain volumetric flow rate up to a maximum of 3.5 l/min, was calibrated before use. The ultrasonic transducer had a probe tip diameter of 22 mm. The horn was immersed to a fixed depth of 3 cm below the air–water interface inside the jacketed glass flow reactor (sonication vessel) which had approximate internal dimensions of 4 cm internal diameter and 10 cm height. Temperature was measured using a Pt100 probe.

2.3. Methods

A summary of the experimental conditions is shown in Table 1. In a typical run, two grams of alumina particles were suspended in the vessel containing deionized water to which ultrasound was applied for the duration of 10 min. The total volume of the suspension in the system was 750 ml. The particle size in the form of mean chord length (ℓ_m) was monitored in-line using the FBRM probe for the full duration of the experiment. The particle suspension was pumped from the sonication vessel (A) to the FBRM beaker (F) and circulated back to the sonication vessel (A). Agitation in the FBRM beaker was kept fixed at 400 rpm. The agitator in the FBRM beaker had negligible effect on the particle breakage as verified by monitoring the particle size change under agitation over a long period of time. A similar test was performed confirming the negligible effect of the peristaltic pump on particle breakage. The sonication and hence the run was started after a period of pumping that allowed the particles to suspend throughout the flow homogenously. FBRM particle size data and ultrasound transducer data were collected using two separate computers. The temperature probe was also connected to the computer recording temperature continuously. At the end of the run, a sample was withdrawn iso-kinetically for microscopic analysis which was carried out using a field emission scanning electron microscope (JOEL, JSM6700F, Japan).

Table 1
Details of experimental runs

Experiment no.	Amplitude ratio	Rated input power (W)	Volumetric flow rate (ml.min^{-1})	Temperature (C)
1	0.3	150	1600	10 ± 3
2	0.3	150	1600	17 ± 2
3	0.3	150	1600	25 ± 2
4	0.3	150	1600	37 ± 1
5	0.3	150	1600	50 ± 1
6	0.5	250	1600	10 ± 2
7	0.5	250	1600	17 ± 1
8	0.5	250	1600	25 ± 2
9	0.5	250	1600	37 ± 1
10	0.5	250	1600	50 ± 1
11	0.7	350	1600	10 ± 3
12	0.7	350	1600	17 ± 2
13	0.7	350	1600	25 ± 1
14	0.7	350	1600	37 ± 1
15	0.7	350	1600	50 ± 1
16	0.7	350	1000	25 ± 1
17	0.7	350	2200	25 ± 1
18	0.9	450	1600	10 ± 3
19	0.9	450	1600	17 ± 2
20	0.9	450	1600	37 ± 1
21	0.9	450	1600	50 ± 1

2.4. Particle size measurement

Focused beam reflectance method is an in-situ method for determining the chord length (CLD) distribution of a suspension with low to high solids concentration [18]. A focused monochromatic infrared laser beam rotates at a fixed high speed and the backscattered/reflected light signals from the surfaces of thousands of particles intersected by the laser light are captured. The time interval (Δt) between signals from the two edges of a particle is converted to chord length (s) by:

$$s = v_b * \Delta t \quad (1)$$

Where v_b is beam velocity. Because tens of thousands of such chord lengths are measured each second, a statistically representative CLD of the particle system under investigation is generated. Fig. 2 illustrates the measurement procedure.

The FBRM is a well established technique that has been used to monitor size distributions [19–21] in crystallization as well as in biotechnology [22,23], amongst other applications. Recently, Kovalsky et al. used this technique for on-line characterization of floc size and structure [24]. They used Fourier transform of the unprocessed signal (i.e., the reflected signal) to arrive at the mass fractal dimensions of the flocs. It is also claimed that apart from size and shape, the unprocessed reflected signals could also yield information on particle texture. The CLD can be converted to particle size distribution by an ill-posed inverse problem

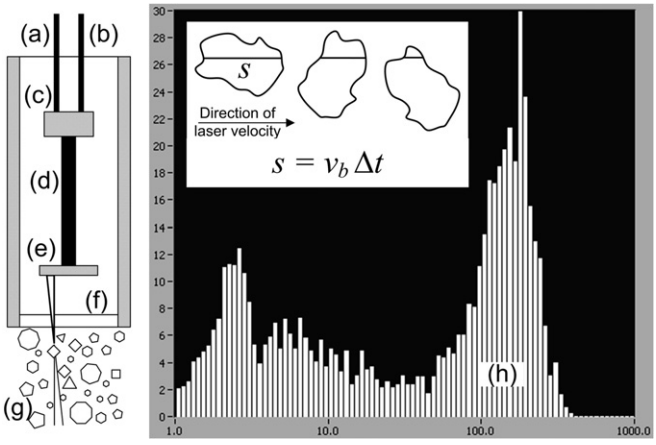

Fig. 2. Particle size measurement using FBRM. (a) laser diode, (b) detector, (c) beam splitter, (d) laser beam, (e) optics rotating at fixed high velocity, (f) sapphire window, (g) particles, and (h) typical chord length distribution.

which can be tackled by constrained least squares minimization procedure or by method of projection onto convex sets [18]. Throughout this work, we characterize particle size and hence breakage by HIU in terms of chord lengths rather than typical particle size. The motivation for this lies in the reliability of the measurement technique as well as in the fact that decreasing chord length is a direct indication of fragmentation. Further, we are interested in identifying the number counts, a measure readily generated by the FBRM.

The probe was inserted in the FBRM beaker that has flow from and to the sonication vessel. Such monitoring in the in-line mode was necessary firstly because the sonication vessel cannot accommodate the FBRM probe and secondly, because it was necessary to keep the FBRM probe at a safe distance from the intense ultrasound field.

3. Results and discussion

As described above, the variation of mean chord length (ℓ_m) of the breaking particles was continuously monitored with sonication time. There was a steady decrease in ℓ_m with increase in sonication time. This is true for all input power levels and temperatures.

3.1. Effect of input ultrasonic power

The experiments were conducted at three different rated input power levels of 150 W, 250 W and 350 W (amplitude ratios of 0.3, 0.5 and 0.7, respectively). The CLD was monitored in-line while the sonication was performed. The cumulative undersize distributions at the start and end of each experiment are summarized in Fig. 3. A decrease in ℓ_m was observed for all input power levels. A higher percentage decrease was observed for higher input power with 350 W of input power showing the highest decrease in ℓ_m for the constant sonication time of 10 min. We also report the temporal variation of ℓ_m under different input power and at the constant temperature and volumetric flow of 25 °C and 1.6 l/min, respectively. The following time-varying dimensionless number, mean chord length ratio (MCLR) is used here and is expressed as:

$$\mathrm{MCLR}(t) = \frac{\ell_m(t)}{\ell_0} \tag{2}$$

where ℓ_0 is the mean chord length in (μm) at the start ($t = 0$) of the experiment.

It is clearly evident from the cumulative distributions and MCLR data that there is breakage of particles occurring during sonication. Furthermore, it can be observed from the cumulative distribution plots that the gap between the $t = 0$ and $t = 10$ min distributions is the highest for 350 W of rated input power and lowest for 150 W. These results indicate higher breakage of particles with increase in input ultrasonic power.

Fig. 4 shows the variation of MCLR under the three amplitude ratios studied. It is evident that an amplitude ratio of 0.7 corresponding to a rated input power of 350 W leads to the highest level of breakage, whereas, amplitude ratio of 0.3 corresponding to rated input power of 150 W results in the lowest breakage. However, one should take care when interpreting this graph, as it could be misleading. This is because, higher total input power does not necessarily mean that the operation is at the optimum as far as efficiency is concerned. It is clear from Fig. 4 that if more power is input into the system, more particle breakage occurs. However, this alone does not indicate optimum input power. Here one needs to quantify the efficiency of conversion of ultrasound energy into breakage (η_b) to arrive at a meaningful optimum. This efficiency determination is discussed in Section 3.4. From Fig. 4, it is also evident that, if time is the optimizing variable, then, operating at higher input power represents the best viable option because it breaks and thus reduces the particle size faster (see Fig. 14 and related discussion in Section 3.4.4 below). In situations where time is not the constraint but

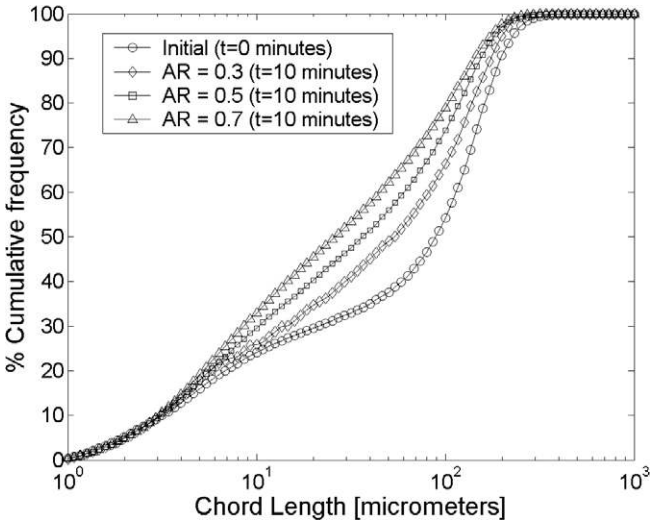

Fig. 3. The cumulative undersize distributions at the start and end of 10 min of sonication for amplitude ratios of 0.3, 0.5 and 0.7, temperature = 25 °C, volumetric flow rate = 1.6 l/min.

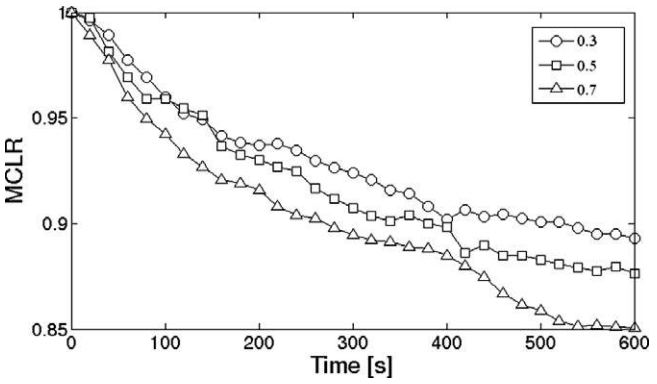

Fig. 4. Variation of MCLR at amplitude ratios of 0.3, 0.5, 0.7, temperature = 25 °C, volumetric flow rate = 1.6 l/min.

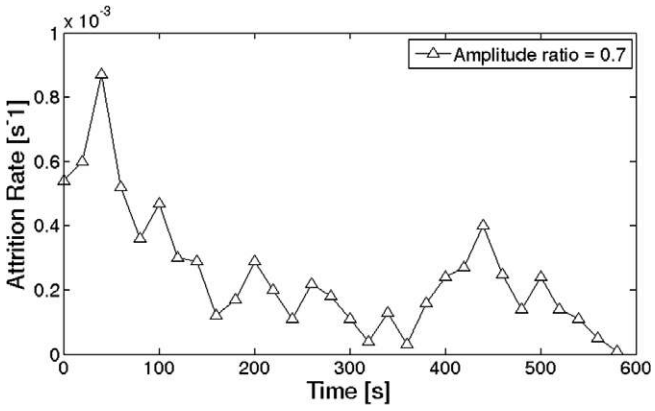

Fig. 5. Breakage rate vs. time, amplitude ratio = 0.7, temperature = 25 °C, volumetric flow rate = 1.6 l/min.

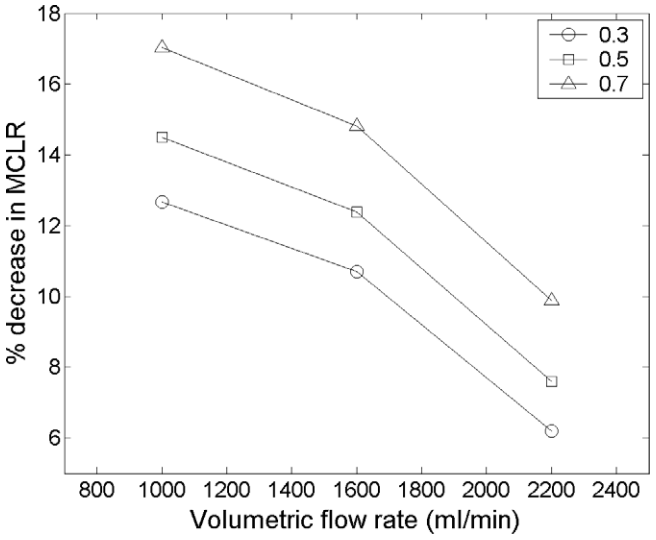

Fig. 6. Percentage decrease in MCLR at different volumetric flow rates, for amplitude ratios, temperature = 25 °C. Data points joined to indicate trends.

energy is the one to be optimized, then it is immaterial as to which input power one operates at, since to achieve the same level of size reduction the higher input power requires the same energy as that of a lower input power operation. The only difference being in the time taken to reach the reduced size.

We further determine the variation of the rate of change of MCLR to gain some insights into breakage kinetics of particles subjected to HIU fields. The breakage rate (K_b) is defined as,

$$K_b \delta t = 1 - \mathrm{MCLR} \tag{3}$$

Fig. 5 shows the change of K_b with sonication time for amplitude ratio of 0.7 and at a temperature of 25 °C. Similar results were obtained for other power levels and temperatures.

Fig. 5 shows a general decrease in K_b. This suggests that K_b is a function of the particle size. The breakage rate decreases as the experiment progresses proportionally correlating to particle size decrease which is also true for any grinding process. Furthermore, this implies that the breakage distribution functions would have strong dependance on particle size. Similar results were obtained for other amplitude ratios as well.

3.2. Effect of contact time

The experimental setup in its continuous flow arrangement allowed the variation of the mean residence time (contact time) of the particles by varying the pump flow rate. Three different flow rates were studied; 1.0 l/min, 1.6 l/min and 2.2 l/min. Breakage was more prominent at lower flow rates corresponding to larger values in residence time. Fig. 6 shows that as residence time increases, particle breakage is enhanced. This is explained as follows: as the residence time increases, the particles spend more time in contact with the breakage forces of the HIU field. It is interesting to observe from Fig. 6 that by changing residence times, it was possible to achieve significant improvement in the breakage. We observed a decrease in particle size by 10% within the first 5 minutes of comminution for 2.2 l/min whereas for 1.0 l/min, we observed a decrease of about 17% for the same time period. This is significant because this was not similarly achievable by changing the input power to the system as shown in Fig. 4. It can be said that from an operational design point of view, changing the flow rate would be a better option for achieving optimum performance. This is the case where comminution time is not constrained. If comminution time is to be optimized, then input power needs to be taken into account as discussed previously in Section 3.1. We also analyzed the breakage rate under different flow rates and obtained results similar to those shown in Fig. 5. We do not show these here to avoid repetition.

3.3. Effect of temperature

Five different experiments were conducted each at one temperature in the range 10–50 °C, at a constant flow rate of 1.6 l/min and each was repeated at all the three amplitude ratios of 0.3, 0.5 and 0.7. Fig. 7 shows the clear trend of the influence of temperature on breakage. Breakage continues to occur as the experiment progresses, but a higher breakage value is shown to exist at an optimum in the temperature range. The breakage (in terms of percentage decrease in ℓ_m) as measured at the end of 10 min of continuous sonication is shown in Fig. 8. This identifies the optimum temperature to be between 25 °C and 37 °C corresponding to the highest percentage decrease of about 15%. The influence of input power on the percentage decrease in ℓ_m is also shown in Fig. 8 and it corroborates with the discussion in 3.1.

Temperature has a significant effect on the cavitation phenomenon. The cavitation phenomenon in a liquid medium is affected by its surface tension, viscosity and vapor

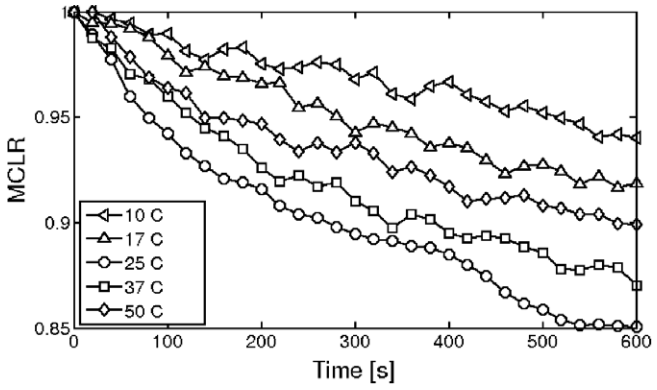

Fig. 7. Variation of MCLR at different temperatures, amplitude ratio = 0.7, volumetric flow rate = 1.6 l/min.

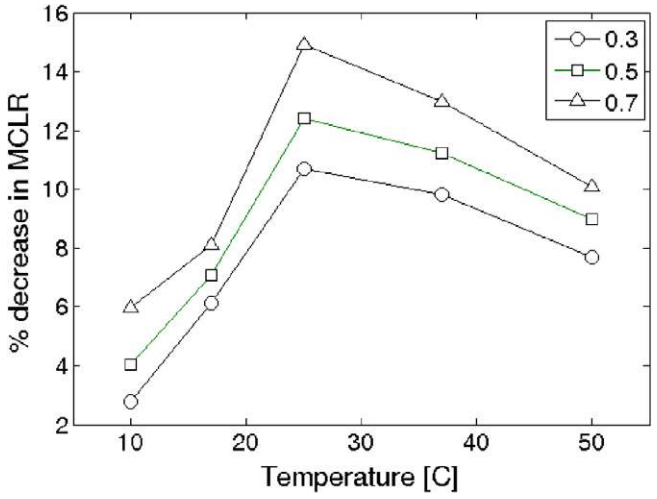

Fig. 8. Percentage decrease in MCLR at different temperatures and amplitude ratios. Data points joined to indicate trends.

pressure [1,4]. Increasing temperature results in reduction in acoustic cavitation threshold, meaning, the liquids cavitate at lower intensities [4]. This can be attributed to the increase in vapor pressure of the liquid when temperature is raised. The increase in temperature results in decrease in surface tension, again aiding in the reduction of the cavitation threshold. Moreover, increasing the temperature reduces the viscosity of the liquid medium. The decrease in viscosity decreases the magnitude of the natural cohesive forces acting on the liquid, and thus, decreases the magnitude of the cavitation threshold. Lower cavitation thresholds translate into ease of cavity formation, thereby making higher temperatures more favorable for particle breakage. Thus, the effect of temperature constitutes three mechanisms that all lead to enhanced cavitation inception, which in turn enhance the breakage. This discussion assumes that it is the high speed micro-jets emanating from the asymmetric transient cavitation collapse that cause the breakage [6]. This is the reason, why we observe an increase in breakage of particles as temperature is varied from 10 °C to 25 °C. As temperature is increased beyond 25 °C, we observe a decrease, contradicting the current discussion on the temperature effect. This can be explained as being primarily caused by the cushioning effect of increased cavity internal vapor pressure at higher temperatures [4]. Due to this cushioning effect, the intensity of the collapse and subsequently the breakage decreases after 25 °C. There are thus, two opposing factors that are at play during the particle breakage; the first is the increase in the number of cavitation events with increase in temperature and due to which particle breakage increases; the second is the cushioning effect of the cavity internal vapor pressure which has a suppression effect on the cavitation intensity and subsequently on particle breakage. It is the relative magnitude of these two opposing effects which dictates the variation of breakage characteristics with temperature as seen in Fig. 8. The former factor is dominant in regions of temperature near and below 25 °C, while the latter becomes more dominant as temperature moves above 25 °C.

This is consistent with the variation of cavitation erosion with temperature observed elsewhere [25–28]. This suggests that two factors are important as far as the particle breakage is considered viz., the size of active cavitation zone and the effect of vapor pressure. The former increases with increase in temperature while the latter decreases, resulting in a negative effect.

3.4. Efficiency of ultrasound energy conversion

It is well known that the amount of energy or power that is input to the system is never completely transferred to the liquid medium and that losses are inherent in the system. Here we analyze efficiency to understand this and attempt to determine optimal operational conditions for particle breakage.

3.4.1. Efficiency of power transfer

We first study the transfer of power or energy into the liquid medium from the ultrasonic transducer at various amplitude ratios and temperatures using calorimetry where the specific calorimetric power is given by,

$$P_{\mathrm{cal}} = m_{\mathrm{L}} \cdot C_{\mathrm{P}} \cdot \left(\frac{\partial T}{\partial t}\right)_{t=0} \tag{4}$$

where P_{cal} is the calorimetrically determined power (W), C_{P} is the specific heat capacity of liquid (kJ kg^{-1} °C^{-1}) and $\left(\frac{\partial T}{\partial t}\right)_{t=0}$ is the rate of change of the uncontrolled system temperature at the start of sonication. Specific input power can be determined by knowing the volume V (m^3) of the sonicated liquid,

$$P_{\mathrm{cal}}^{\mathrm{sp}} = \frac{P_{\mathrm{cal}}}{V} \tag{5}$$

Thompson and Doraiswamy [1] modified this expression to account for the heat transferred to the jacket or the vessel. The calorimetric power (P_{cal}) was calculated for different amplitude ratios and at different bulk fluid temperatures. The energy transferred from the frequency generator to

the ultrasonic transducer, termed here P_h, was measured by the in-built watt-meter which gave the amount of energy transferred in watts. The efficiency of power transfer η_{PT} was calculated for the different tested input powers and temperatures and is here defined after Loning et al. [15] as

$$\eta_{PT} = \frac{P_{cal}}{P_h} \tag{6}$$

It is evident from the results shown in Fig. 9 that P^{sp}_{cal} is dependent on the temperature of the system. There is a marginal decrease in P^{sp}_{cal} with increase in temperature consistent with the findings of Loning et al. [15].

Furthermore, there is a linear variation of P^{sp}_{cal} with amplitude ratio (Fig. 10), contradictory to previous work [29] where a quadratic variation was reported while being in agreement with others [14] who reported similar linear findings. Our experimental results add more weight to the claim that a linear variation of P_{cal} with amplitude ratio is more realistic for the cavitations under the horn tip.

Fig. 11 shows the variation of η_{PT} with amplitude ratio and temperature. A marginal decrease of η_{PT} is observed

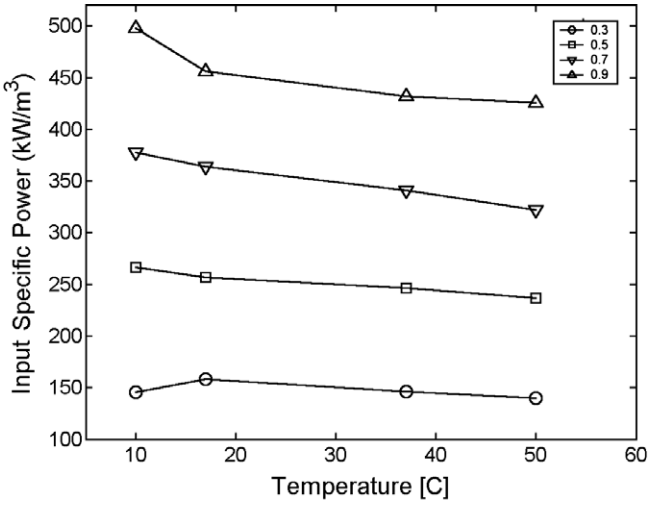

Fig. 9. Variation of P^{sp}_{cal} (kW m^{-3}) with temperatures at different amplitude ratio. Data points joined to indicate trends.

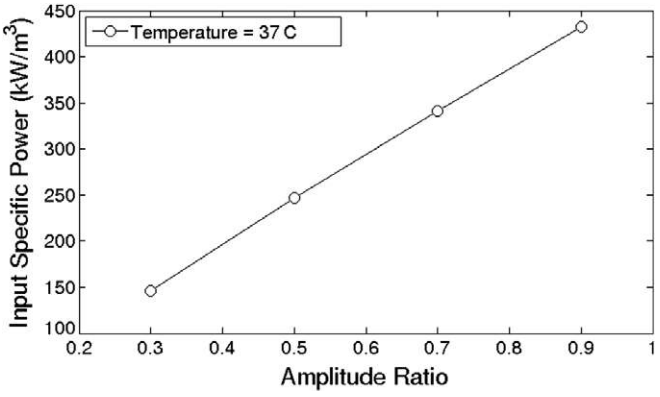

Fig. 10. Variation of P^{sp}_{cal} (kW m^{-3}) with amplitude ratio, temperature = 37 °C.

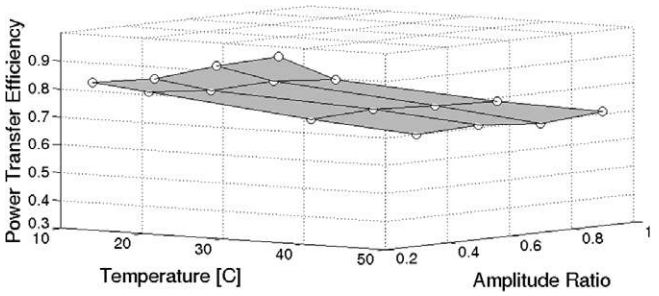

Fig. 11. Variation of η_{PT} from horn to liquid medium with temperature and amplitude ratio.

with increase in temperature and η_{PT} is found to be independent of the amplitude ratio. This suggests that the properties of the medium influence the amount of energy transferred to it [15] and that the amount of power transferred has no influence on the η_{PT}. It is to be noted, however, that this efficiency does not include the energy losses that occur during transfer of power from the electrical supply to the frequency generator.

3.4.2. Efficiency of ultrasound energy conversion to particle breakage

In the previous section, we calculated the efficiency of the power transfer from the ultrasonic transducer to the thermal energy of the liquid. Now, the efficiency of ultrasound energy conversion to particle breakage (η_b) is calculated. The energy that is input to the suspension by means of ultrasound horn vibrations (P_h) is transferred to energy for breakage (P_b), heat energy (P_{heat}) and other losses (to the ambient air, acoustic streaming, sonoluminescence, etc) (P_{losses}). The ultrasonic energy flow path [15] can be mapped in the following way

$$P_h \rightarrow P_{cal} \tag{7}$$

$$P_{cal} = P_b + P_{heat} + P_{losses}, \tag{8}$$

where P_{heat} (W) is given by the expression

$$P_{heat} = m_L \cdot C_P \cdot \left(\frac{\partial T}{\partial t}\right)_{breakage, t=0} \tag{9}$$

P_{heat} is obtained by monitoring the uncontrolled temperature rise continuously in the presence of breakage activity (i.e., when particles are being sonicated). If the P_{losses} is negligible to the energy expended in particle breakage, then without the loss of generality, the efficiency of conversion of energy input to the desired mechanical effect (in this case, particle breakage) is conveniently given by

$$\eta_b = 1 - \frac{P_{heat}}{P_{cal}} \tag{10}$$

It is important however, to realize that the acoustic nature of the ultrasonic field is altered when particles are suspended in the medium. Further, higher particle loading levels influence the efficiency of η_{PT} due to the change in the viscosity of the medium. We use a low particle loading

(two grams in 750 ml of water), such that the ultrasonic field is not attenuated to any significant extent. This information of variation of η_b with amplitude ratios and temperature will be helpful for scale-up and design purposes.

Finally, the net efficiency (η_{net}) of ultrasound energy conversion to particle breakage can be obtained by

$$\eta_{net} = \eta_{PT} \cdot \eta_b \tag{11}$$

3.4.3. Variation of η_b and η_{net} with temperature

Fig. 12 shows that η_b increases with increase in temperature up to 25 °C and thereafter decreases. The main reason for the increase in η_b with increase in temperature is the increase in number of cavitation events as discussed previously. The increase observed initially is followed by decrease in collapse intensity above 25 °C due to the increase in the vapor pressure. This causes η_b to decrease at higher temperatures. Similar results are obtained for all amplitude ratios tested. It is interesting to observe that the same trend in efficiency change due to temperature change is not observed for chemical effects like radical formation. In such processes, a decrease in energy yield is obtained with increase in temperature [14]. It is suggested that for optimal operations, where both mechanical and chemical effects take place, a trade-off is necessitated which makes intermediate temperatures the most viable option. Such a scenario includes solid–liquid reactions where reaction rate is augmented by the breakage of solid particles increasing the surface area that enhances dissolution [30]. The net efficiency (η_{net}) is shown, in Fig. 12, to behave in the same way as η_b.

3.4.4. Variation of η_b with amplitude ratio

Fig. 13 shows that η_b is almost constant with increase in amplitude ratio. This indicates that, even though there is an increase in cavitation events with increase in the amplitude ratio, the increase is at the expense of greater energy input

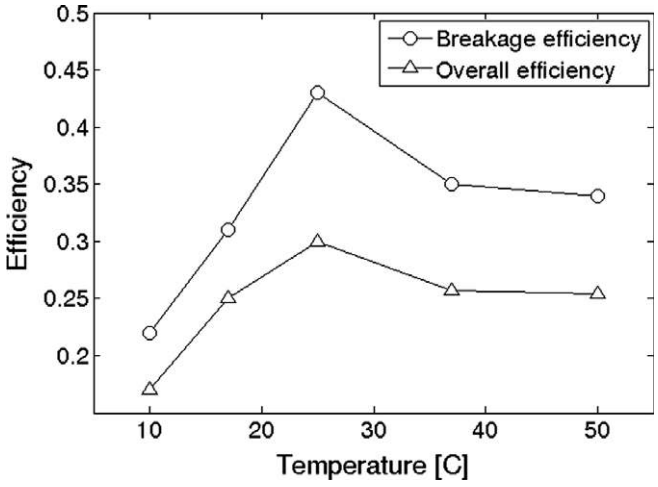

Fig. 12. Variation with temperature of breakage efficiencies, amplitude ratio = 0.7, volumetric flow rate = 1.6 l/min. Data points joined to indicate trends.

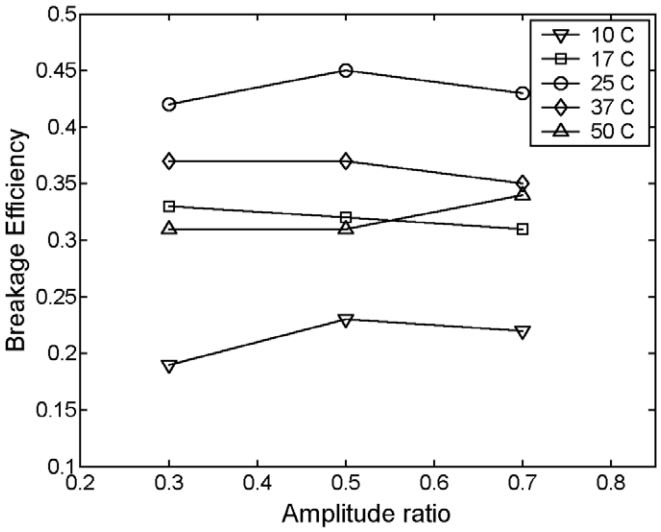

Fig. 13. Variation with amplitude ratio of η_b at different temperatures. Data points joined to indicate trends.

to the system. In effect, no change in efficiency is obtained by merely increasing the magnitude of input power. This is corroborated by data in Fig. 14 which shows the MCLR, for the different amplitude ratios, against E_m which is the total energy input (E_{Tot}) to the system (from the frequency generator) per unit mass of particles m_p to be comminuted, given by

$$E_m = \frac{E_{Tot}}{m_p} \tag{12}$$

It is evident from Fig. 14, that as the E_m is increased, more breakage is obtained. For amplitude ratio of 0.7, more energy is input to the system at a constant sonication time, so naturally higher breakage is expected and observed. Conversely, at the lower amplitude ratio of 0.3, less energy is input for the same sonication time and so less breakage is observed. If at all, there had been variation in η_b with amplitude ratio, then for the same amount of input energy and for a same sonication time interval, different breakage would have been observed for different amplitude ratios,

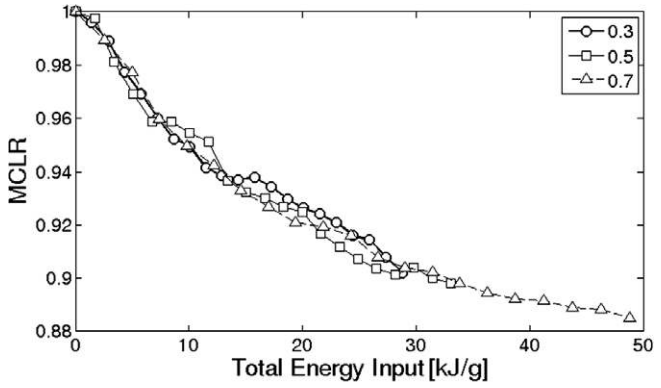

Fig. 14. Variation of MCLR vs. E_m, at various amplitude ratios for a time interval of 400 s, temperature = 25 °C, volumetric flow rate = 1.6 l/min.

resulting in the three curves of Fig. 14 being dispersed apart. The almost superposition here of the data concludes that η_b is independent of the amplitude ratio.

3.5. Surface morphology of the sonicated particles

Figs. 15 and 16 compare the SEM images of Al_2O_3 particles before and after sonication. Fig. 16 clearly shows the effect of HIU fields which has transmuted the whole surface morphology of the particles. Under the effect of all input power levels, samples showed similar surface morphologies, with varying relative magnitudes for different power levels.

There are many crater-like surface irregularities formed. The whole surface of the particle has "battered sponge" like irregularities. Creation of such surface morphology by HIU could be exploited in catalysis. As far as catalysis is concerned, there are two main features of catalytically active surfaces that are imperative viz., (a) irregularities and (b) additives. The steps and kinks that appear on metal surfaces seem to have an enhancing effect, especially for transition metal surfaces [31]. However, creation of regular step and kink pattern on metal surface by HIU would be a formidable task, nevertheless, if mesoporous catalysts need to be designed with increased pore volume and higher surface area, then, ultrasound would indeed be a viable option. The past efforts of utilizing the cavitation erosion phenomenon in catalysis were mostly directed at characterizing the wear resistance of a particular material. It has been reported that sonication and subsequent processing techniques can be used to create nano-sized alumina catalyst particles with a controlled mesoporous distribution [32].

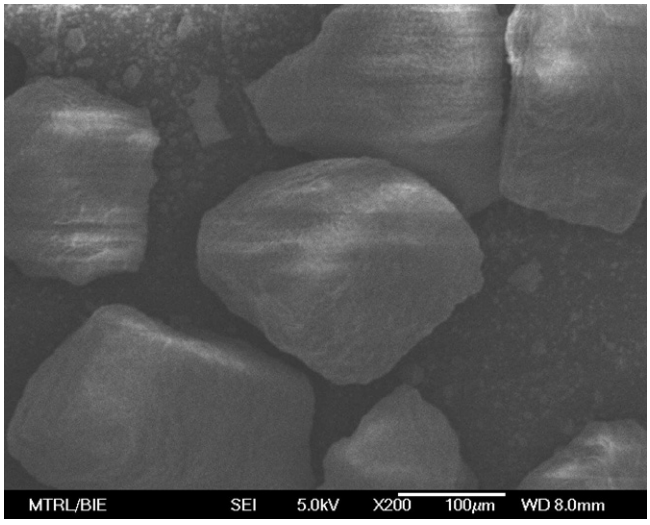

Fig. 15. SEM micrograph of Al_2O_3 particles – before sonication.

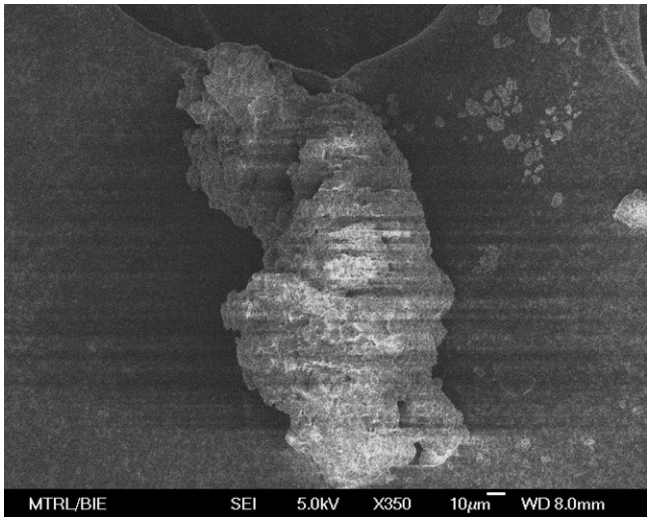

Fig. 16. SEM micrograph of Al_2O_3 particles after 10 min of sonication, amplitude ratio of 0.7, temperature = 25 °C for 10 min.

4. Conclusions

The ultrasound mediated particle breakage was investigated experimentally using a continuous flow sonication apparatus equipped with in-line FBRM particle size monitoring. The effects of sonication power, contact time and temperature of the bulk liquid on the particle breakage were discussed. Higher sonication power and higher contact time result in higher breakage. Breakage rate was quantified and was found to be highest in the initial period of sonication. An optimum temperature corresponding to higher breakage was found to exist in the range 25–37 °C. Temperature affects the particle breakage by increasing the size of the cavitation zone as well as increasing the vapor pressure, both of which have opposing influences, where the former was found to enhance breakage. There is a marginal decrease in efficiency of power transfer from horn to liquid with increase in temperature. The efficiency of ultrasound energy conversion to particle breakage was calculated using calorimetry and found along with the net efficiency to initially increase with temperature and then decrease after reaching a maximum at about 25 °C. Preliminary scanning by electron microscopy was performed yielding invaluable information on the "battered sponge" like surface irregularities caused due to HIU fields. However, further methodological study is warranted to establish the breakage mechanisms.

Acknowledgements

The authors thank Pauline Yeo and Poernomo Gunawan for their technical assistance. The authors also gratefully acknowledge the help of Dr. Brain O'Sullivan and Assistant Professor Arvind Rajendran in reviewing the manuscript.

References

[1] L. Thompson, L. Doraiswamy, Sonochemistry: Science and engineering, Industrial and Engineering Chemistry Research 38 (1999) 1215–1249.

[2] P. Chendke, H. Fogler, Second-order sonochemical phenomena-extensions of previous work and applications in industrial processing, The Chemical Engineering Journal 8 (1974) 165–178.
[3] Y. Ichida, R. Sato, Y. Morimoto, K. Kobayashi, Material removal mechanisms in non-contact ultrasonic abrasive machining, Wear 258 (2005) 107–114.
[4] T. Mason, J. Lorimer, Applied Sonochemistry: The Uses of Power Ultrasound in Chemistry and Processing, Wiley-VCH Verlag GmbH and Co. KGaA, 2002.
[5] S. Thoma, M. Ciftcioglu, D. Smith, Determination of agglomerate strength distributions: Part 1. Calibration via ultrasonic forces, Powder Technology 68 (1991) 53–61.
[6] K. Suslick, D. Casadonte, M. Greent, M. Thompson, Effects of high-intensity ultrasound on inorganic solids, Ultrasonics 25 (1987) 56–59.
[7] R. Zhao, J. Goodwin, R. Oukaci, Attrition assessment for slurry bubble column reactor catalysts, Applied Catalysis A: General 189 (1999) 99–116.
[8] D. Bukur, Attrition studies with catalysts and supports for slurry phase Fischer-Tropsh synthesis, Catalysis Today 106 (2005) 275–281.
[9] P. Sanchez-Soto, A. Wiewiora, M. Aviles, A. Justo, L. Perez-Maqueda, J. Perez-Rodriguez, P. Bylina, Talc from Puebla de lillo, Spain. Part 1. Effect of dry grinding on particle size and shape, Applied Clay Science 12 (1997) 297–312.
[10] L. Perez-Maqueda, A. Duran, J. Perez-Rodriguez, Preparation of submicron talc particles by sonication, Applied Clay Science 28 (2005) 245–255.
[11] U. Teipel, K. Leisinger, I. Mikonsaari, Comminution of crystalline material by ultrasonics, International Journal of Mineral Processing 74 (2004) S183–S190.
[12] M. Kass, Ultrasonically induced fragmentation and strain in alumina particles, Materials Letters 42 (2000) 246–250.
[13] T. Kimura, T. Sakamoto, J. Leveque, H. Sohmiya, M. Fujita, S. Ikeda, T. Ando, Standardization of ultrasonic power for sonochemical reaction, Ultrasonics Sonochemistry 3 (1996) S157–S161.
[14] M. Kuijpers, M. Kemmere, J. Keurentjes, Calorimetric study of the energy efficiency for ultrasound-induced radical formation, Ultrasonics 40 (2002) 675–678.
[15] J. Loning, C. Horst, U. Hoffmann, Investigations on the energy conversion in sonochemical processes, Ultrasonics Sonochemistry 9 (2002) 169–179.
[16] J. Loning, C. Horst, U. Hoffmann, in: Seventh Meeting of the European Society of Sonochemistry (2000) 197.
[17] P. Lickiss, The New Chemistry, Cambridge University Press, Cambridge, 2000.
[18] J. Worlitschek, Monitoring, modeling and optimization of batch cooling crystallisation, Ph.D. thesis, Swiss Federal Institute of Technology, Zurich (2003).
[19] P. Schirg, P. Wissler, Membrane processes for the chemical and pharmaceutical industry and optimization of particulate processes by lasentec FBRM, Chimia 54 (2000) 207–210.
[20] P. Barrett, B. Glennon, In-line monitoring of crystal growth in batch crystllization operations, in: Proceedings of the Fourteenth International Symposium on Industrial Crystallization, Cambridge (1999) 12–16.
[21] O. Monnier, G. Fevotte, C. Hoff, J. Klein, Model identification of batch cooling crystallizations through calorimetry and image analysis, Chemical Engineering Science 52 (1997) 1125–1139.
[22] K. McDonald, A. Jackman, S. Hurst, Characterization of plant suspension cultures using the focused beam reflectance technique, Biotechnology Letters 23 (2001) 317–324.
[23] P. Barrett, B. Glennon, In-line FBRM monitoring of particle size in dilute agitated suspensions, Particle Systems Characterization 16 (1999) 207–211.
[24] P. Kovalsky, G. Bushell, In situ measurement of fractal dimension using focused beam reflectance measurement, Chemical Engineering Journal 111 (2005) 181–188.
[25] M. Plesset, Temperature effects in cavitation damage, Journal of Basic Engineering 94 (1972) 559–566.
[26] S. Hattori, Y. Tanaka, Influence of air content and vapor pressure of liquids on cavitation erosion, Trans. JSME 68 B (2002) 130–136.
[27] S. Hattori, Y. Goto, T. Fukuyama, Influence of temperature on erosion by a cavitating liquid jet, Wear 260 (2006) 1217–1223.
[28] C. Kwok, H. Man, L. Leung, Effect of temperature, pH and sulphide on the cavitation erosion behaviour of super duplex stainless steel, Wear 211 (1997) 84–93.
[29] T. Leighton, The Acoustic Bubble, 1st ed., Academic Press, 1997.
[30] A. Kannan, S. Rathan, Enhancement of solid dissolution process, Chemical Engineering Journal 102 (2004) 45–49.
[31] G. Somorjai, Catalysis and surface science, Surface Science 89 (1979) 496–524.
[32] N. Yao, G. Xiong, S. Sheng, M. He, W. Yang, X. Bao, Ultrasound as a tool to synthesize nano-sized silica-alumina catalysts with controlled mesoporous distribution by a novel sol-gel process, Catalysis Letters 78 (2002) 37–41.